Scientia Iranica, Vol. 15, No. 3, pp 286–294

SCIENTIA IRANICA

A Method for Calculation of Face Gradients in Two-Dimensional, Cell Centred, Finite Volume Formulation for Stress Analysis in Solid Problems

N. Fallah[1]

In this paper, a procedure is proposed for the evaluation of displacement gradients in a two-dimensional, cell centred, finite volume formulation for stress analysis in linear elastic solid problems. Temporary elements with isoparametric formulations are used for calculation of the gradients at the cell boundaries. In this way, stress continuity across the common face of the two adjacent cells will be guaranteed. The formulation is verified by three test cases, in which the proposed formulation shows good predictions.

INTRODUCTION

In recent years, there has been growing interest in developing a finite volume discretization approach for solving solid mechanics problems. This is due to the fact that the method is conceptually simple and, also, in the investigated problems, it is seen that the method is able to accurately predict structural behaviours. For instance, it has been observed that the finite volume formulation, based on the Mindlin-Reissner plate theory, behaves well in the bending analysis of thin to thick plates [1]. However, it is known that, due to the so-called shear-locking phenomena, the displacement based finite element formulation is not able to analyze thin Timoshenko plate models discretized by isoparametric elements with linear shape functions, in which full integrations are performed. Hence, in the author's opinion, the application of the method will be extended to more solid-structural problems in the future.

There are different procedures in displacement Finite Volume (FV) methods for the calculation of displacement derivatives on cell boundaries. Demirdzic et al. [2,3] have assumed a linear displacement distribution function across a cell and all of its neighbouring cells, based on a Cell Centred Finite Volume Method (CC-FVM). By averaging the derivatives of the displacement distributions of the two cells with common cell faces, they calculate strains on cell faces. Wheel [4,5] has presented an approach, based on the CC-FVM, in which a linear distribution of displacements across each cell face has been assumed. Then, displacement derivatives have been obtained by applying the central difference scheme in a skew coordinate system. Bailey and Cross [6] in the Cell Vertex Finite Volume Method (CV-FVM), also called as the Finite Element Finite Volume (FE-FV) method, have used the control volumes formed over the conventional FE mesh by connecting the element centres to the midpoints of the element faces. In this approach, for two-dimensional analysis, the solution domain is discretized by 3-node triangles or 4-node quadrilateral isoparametric elements and, for three-dimensional analysis, 8-node isoparametric hexahedral elements are used. Bilinear shape functions have been used for the interpolation of unknown variables and element geometry within the elements. To approximate the gradient of displacements at the middle of a given cell face, the calculation is performed in the natural space of the enclosing element and then mapped back to the global coordinate system. Approximating the gradients in this manner is a well-structured procedure, which has been applied for the modelling of different solid problems [7-9]. It should be noticed that, in the above works, the solution domain is discretized by using isoparametric elements only. The advantages and disadvantages of constructing the control volumes in the ways presented above can be found in [10].

This paper aims to present a procedure for the calculation of face gradients in a cell centred finite volume framework. This approach has similarities

1. *Department of Civil Engineering, University of Guilan, P.O. Box 3756, Rasht, Iran. E-mail: fallah@guilan.ac.ir*

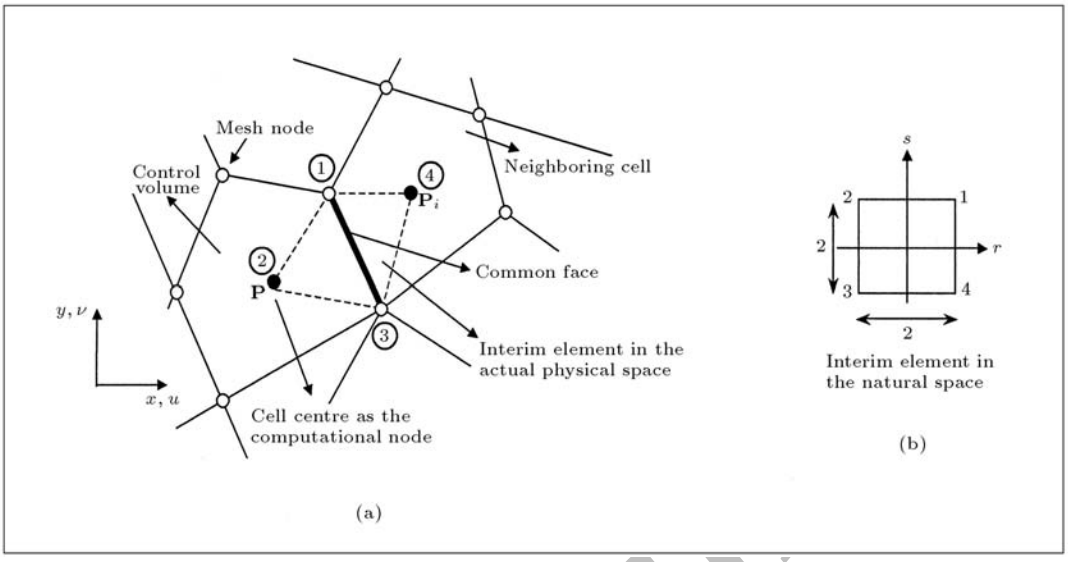

Figure 1. Control volume and an interim element on a control volume's face.

with the method used in CV-FVM. In the presented approach, for the calculation of gradients at a face of the cell, a 4-node temporary element is formed that surrounds the face. The temporary element is, henceforth, referred to as the interim element, since it is used only as a temporary tool for the evaluation of displacement gradients at the enclosed face, after which it is discarded. For a given face, the vertices of an interim element are the centres of the two adjacent control volumes lying on either side of the face and the nodes at each end of the face. The geometry of an interim element and the unknown variables are interpolated within the element by using interpolation functions, which are expressed in the natural coordinate system of the element. Moreover, equilibrium equations of a cell are approximated at the evaluation points, which are located in the interim elements. In this way, for the two cells lying on either side of a face, stress continuity will be satisfied at the common face. This is due to using the evaluation points at the same locations, using the same shape functions and using the same nodal values for the evaluation of gradients across the face. One of the advantages of the presented method for the calculation of face gradients is that it can be used for the solution domain discretized by multi-faceted elements, where the CV-FVM approach cannot be used. To illustrate the accuracy and the convergence rate of the proposed method, three test problems are analyzed by use of the presented formulation. The results obtained are compared with the reference results, which are available in the literature. This testing demonstrates the capability of the proposed method in accurate predictions of the deformations and stresses in two-dimensional loaded solids.

FORMULATION

Figure 1 shows a part of a two-dimensional solid body, where the calculation domain is meshed to elements with arbitrary shapes. Each element is now considered a control volume or cell. The control volume's centre is considered at the element centre. In a static analysis, the equilibrium equation expresses the balance of surface and body forces and, for a given internal cell, **P**, which is surrounded by the neighbouring cells, it can be written in the following form:

$$\int_{\Gamma_A} \mathbf{T}\boldsymbol{\sigma} d\Gamma + \int_{\Omega} \mathbf{b} d\Omega = 0, \tag{1}$$

where $\boldsymbol{\sigma}$ is stress vector, matrix $\mathbf{T}$ includes components of the outward unit normal to the boundaries of the cell and $\mathbf{b}$ is the body force per unit volume. The first integral is a surface integral over the faces bounding the cell, denoted by Γ_A, and the second integral is a volume integral over the cell's volume, Ω. In 2-D problems, for a cell with constant thickness and uniformly distributed body force, one has:

$$\int_{\Gamma} \mathbf{T}\boldsymbol{\sigma} dL + \int_{A} \mathbf{b} dA = 0, \tag{2a}$$

where the first integral is a line integral and A is the area of the cell. Stress vector $\boldsymbol{\sigma}$ and matrix $\mathbf{T}$ are as follows:

$$\boldsymbol{\sigma} = \begin{bmatrix} \sigma_x \\ \sigma_y \\ \sigma_{xy} \end{bmatrix}, \qquad \mathbf{T} = \begin{bmatrix} n_x & 0 & n_y \\ 0 & n_y & n_x \end{bmatrix}. \tag{2b}$$

For a cell enclosed with k faces, Equation 2a becomes:

$$\sum_{i=1}^{k} \int_{\Gamma_i} \mathbf{T}\boldsymbol{\sigma} dL + \int_{A} \mathbf{b} dA = 0. \tag{3}$$

The stress components in Equation 3 can be related to the strain components, using the constitutive equation, which is of the following form:

$$\boldsymbol{\sigma} = \mathbf{D}\boldsymbol{\varepsilon}, \tag{4a}$$

where the entries of matrix $\mathbf{D}$ are the elastic coefficients and $\boldsymbol{\varepsilon}$ is the elastic strain vector as follows:

$$\boldsymbol{\varepsilon} = \begin{bmatrix} \frac{\partial u}{\partial x} \\ \\ \frac{\partial v}{\partial y} \\ \\ \frac{\partial u}{\partial y} + \frac{\partial v}{\partial x} \end{bmatrix},$$

$$\mathbf{D} = \frac{E}{1-v^2}\begin{bmatrix} 1 & v & 0 \\ v & 1 & 0 \\ 0 & 0 & \frac{1-v}{2} \end{bmatrix} \text{(for plain stress problems)}. \tag{4b}$$

Substituting Equation 4a into Equation 3 gives the following:

$$\sum_{i=1}^{k} \int_{\Gamma_i} \mathbf{TD}\boldsymbol{\varepsilon} dL + \in t_A \mathbf{b} dA = 0. \tag{5}$$

The equilibrium Equation 5 is exact and no approximation has been introduced so far. In order to evaluate the line integrals in Equation 5, a distribution of displacement has to be assumed. Here, a bilinear distribution of displacement is assumed in a temporary 4-node element, which surrounds each face of the cell. This temporary element is referred to here as the interim element. For a given face, the vertices of the interim element are the centres of the two control volumes lying on either side of the face and the two remaining vertices are the nodes at each end of the face (Figure 1a).

The interim element is considered an isoparametric element, where the geometry and displacement within the element are interpolated, using the interpolation functions in the same way. The interpolation functions are defined in the natural coordinate system of the element [11] in the following form:

$$N_i(r,s) = \frac{1}{4}(1 + r_i r)(1 + s_i s), \qquad i = 1,2,3,4, \tag{6}$$

in which r_i and s_i are the natural coordinates of the ith corner (Figure 1b).

A displacement component, u, can be approximated anywhere within the interim element using the following:

$$u(r,s) = \sum_{i=1}^{4} N_i(r,s) u_i, \tag{7}$$

or, in the matrix form as follows:

$$\mathbf{u} = \mathbf{N}\widetilde{\mathbf{u}}, \tag{8}$$

where $\widetilde{\mathbf{u}}$ is a vector representing the nodal displacements of the interim element and $\mathbf{N}$ includes interpolation functions:

$$\widetilde{\mathbf{u}} = \begin{bmatrix} u_1 & v_1 & u_2 & \cdots & v_4 \end{bmatrix}^T,$$

$$\mathbf{N} = \begin{bmatrix} N_1 & 0 & N_2 & 0 & \cdots & 0 \\ 0 & N_1 & 0 & N_2 & \cdots & N_4 \end{bmatrix}.$$

In order to evaluate the first order derivative of the displacement components, with respect to the global coordinate system, xy, which are presented in the equilibrium Equation 5, the chain rule of differentiation is applied as follows:

$$\begin{bmatrix} \frac{\partial}{\partial r} \\ \\ \frac{\partial}{\partial s} \end{bmatrix} = \begin{bmatrix} \sum_{i=1}^{4} x_i N_{i,r} & \sum_{i=1}^{4} y_i N_{i,r} \\ \\ \sum_{i=1}^{4} x_i N_{i,s} & \sum_{i=1}^{4} y_i N_{i,s} \end{bmatrix} \begin{bmatrix} \frac{\partial}{\partial x} \\ \\ \frac{\partial}{\partial y} \end{bmatrix}. \tag{9a}$$

Or:

$$\frac{\partial}{\partial r_i} = J_{ij} \frac{\partial}{\partial x_j}, \tag{9b}$$

where matrix $\mathbf{J}$ represents the Jacobean operator for the interim element.

Equation 9 can be given in the matrix form as follows:

$$\frac{\partial}{\partial \mathbf{r}} = \mathbf{J} \frac{\partial}{\partial \mathbf{x}}. \tag{10}$$

To map these local derivatives back to global coordinates, the following transformation is used:

$$\frac{\partial}{\partial \mathbf{x}} = \mathbf{J}^{-1} \frac{\partial}{\partial \mathbf{r}}. \tag{11}$$

By using Equations 8 and 11, the derivatives $\frac{\partial u}{\partial x}$, $\frac{\partial u}{\partial y}$, $\frac{\partial v}{\partial x}$ and $\frac{\partial v}{\partial y}$ can be evaluated and, then, the strain displacement relation can be of the following form:

$$\boldsymbol{\varepsilon} = \mathbf{B}\widetilde{\mathbf{u}}, \tag{12}$$

where matrix $\mathbf{B}$ includes derivatives of the shape functions, with respect to the global coordinate system. Substituting Equation 12 into Equation 5, in the absence of body force, gives:

$$\sum_{i=1}^{k} \int_{\Gamma_i} \mathbf{TDB}\widetilde{\mathbf{u}} dL = 0. \tag{13a}$$

The equilibrium Equation 13a can be approximated, corresponding to each face of the cell. To preserve the simplicity of the method, a uniform strain distribution is assumed on each face of the cell. Hence, Equation 13a becomes:

$$\sum_{i=1}^{k}[(\mathbf{TDB}\widetilde{\mathbf{u}})_{IP}L]_i = 0, \tag{13b}$$

where L is the length of the face and the subscript IP denotes a convenient location within the interim element, for the evaluation of Equation 13b. This location is referred to as the evaluation point corresponding to each face of the cell. For a given face, which is enclosed in an interim element, the midpoint of the face and the centre of the interim element can be considered as locations for the evaluation point. Of course, the local coordinates of the evaluation point, i.e. r and s, can be found by mapping from the global coordinates to the natural coordinates of the element as follows:

$$r = f_1(x, y), \qquad s = f_2(x, y). \tag{14}$$

Equation 13b is evaluated at the selected evaluation points for all faces bounding the cell. Vector $\widetilde{\mathbf{u}}$ includes displacement components, corresponding to the centre of cell **P**, the centres of the cells that are adjacent to the cell faces and the displacements at the corner nodes of the cell. To represent Equation 13b in terms of the displacements at the centres of a given cell and the neighbouring cells, only the corner nodal displacements must be eliminated. For a given corner node, q, it can be achieved by assuming a bilinear distribution of displacement across the region whose vertices are the centres of those cells surrounding the corner node (Figure 2). For instance, the variation of the nodal, u, displacement in this region can be assumed as follows:

$$u = ax + by + c, \tag{15}$$

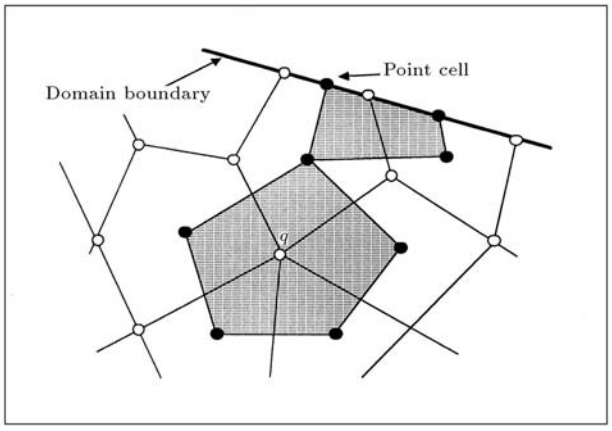

Figure 2. Typical internal and boundary nodes surrounded by regions connecting the centres of the cells lying around.

where the unknown coefficients a, b and c are calculated by ensuring a fit to a set of sampling points, i.e. vertices of the corresponding regions shown in Figure 2. Substituting the coordinates of the sampling points into Equation 15 gives the following:

$$\begin{bmatrix} u_1 \\ u_2 \\ \vdots \\ u_n \end{bmatrix} = \begin{bmatrix} x_1 & y_1 & 1 \\ x_2 & y_2 & 1 \\ \vdots & \vdots & \vdots \\ x_n & y_n & 1 \end{bmatrix} \begin{bmatrix} a \\ b \\ c \end{bmatrix}, \tag{16}$$

or in the compact form:

$$\overline{\mathbf{u}}_q = \overline{\mathbf{x}}_q \mathbf{a}_q. \tag{17}$$

By assuming that the u displacement of the given node, q, is also expressed by Expression 16, one has:

$$u_q = \begin{bmatrix} x_q & y_q & 1 \end{bmatrix} \begin{bmatrix} a \\ b \\ c \end{bmatrix}, \tag{18a}$$

or:

$$u_q = \mathbf{x}_q \mathbf{a}_q. \tag{18b}$$

Eliminating $\mathbf{a}_q$ from Equations 17 and 18b gives the following:

$$u_q = \mathbf{x}_q (\overline{\mathbf{x}}_q^T \overline{\mathbf{x}}_q)^{-1} \overline{\mathbf{x}}_q^T \overline{\mathbf{u}}_q. \tag{19}$$

The nodal v displacement component can be represented in a similar way. The procedure expressed above is applied for all nodes presented in Equation 13b, i.e. the nodes forming the typical cell **P** (Figure 1a). It should be mentioned that the above method is applied in the same manner for the nodes located on the domain boundaries (Figure 2). It is important to notice that the displacement relation of a node and surrounding cell centres depends solely on the mesh geometrical properties. Hence, for a given mesh, an evaluation of Equation 19 is performed only once for each mesh node. The above procedure is similar to the method presented in [5].

After the elimination of the nodal displacements, Equation 13b can be presented in matrix form as follows:

$$\begin{bmatrix} \mathbf{R}_x \\ \mathbf{R}_y \end{bmatrix} [\mathbf{u}] = 0, \tag{20}$$

in which each individual equation represents the relation of displacement components at the centre of cell **P** to those at the centres of the surrounding cells.

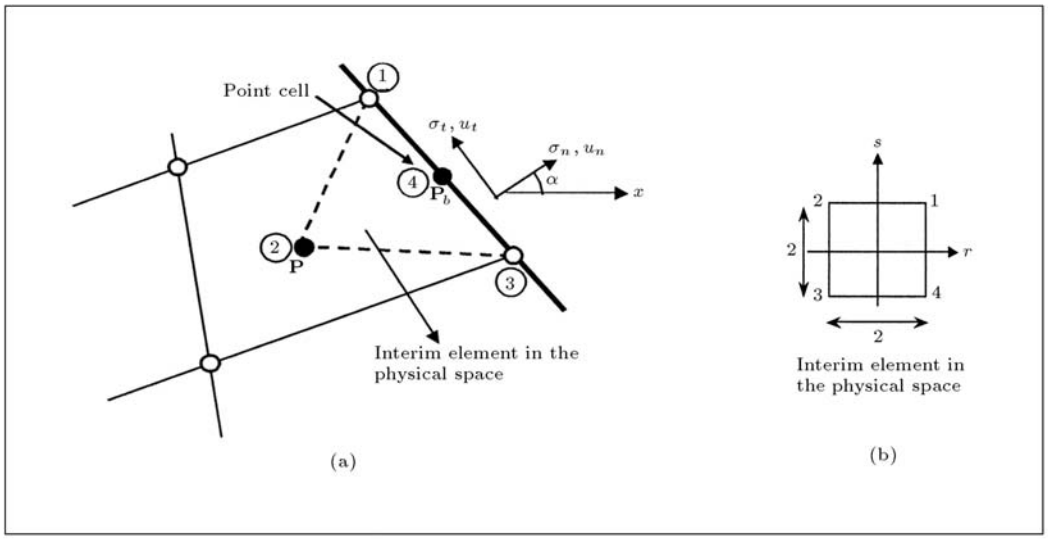

Figure 3. A point cell on the boundary.

BOUNDARY CONDITIONS

To incorporate the boundary conditions into the solution procedures, point cells are used (Figure 3a).

Point cells are considered on the boundaries of the domain, next to the internal cells. For a given internal cell, which is adjacent to the boundary, the corresponding point cell is placed at the middle of the face lying on the boundary, as shown in Figure 3a.

In this way, if displacement boundary conditions are applied, the displacement components of the point cell, $\mathbf{P_b}$, in the global coordinate system, can be obtained from the following:

$$\begin{bmatrix} u \\ v \end{bmatrix}_{P_b} = \begin{bmatrix} \cos\alpha & -\sin\alpha \\ \sin\alpha & \cos\alpha \end{bmatrix} \begin{bmatrix} u_n \\ u_t \end{bmatrix}_{P_b}, \tag{21}$$

in which u_n and u_t are the known normal and tangential components of the applied displacement, respectively. The angle, α, is measured between the outward normal to the boundary face and the x axis.

Moreover, in the case of stress boundary conditions, the applied stress components, σ_n and σ_t, can be represented in the global coordinate system as follows:

$$\begin{bmatrix} \cos^2\alpha & \sin^2\alpha & 2\sin\alpha\cos\alpha \\ -\sin\alpha\cos\alpha & \sin\alpha\cos\alpha & \cos^2\alpha - \sin^2\alpha \end{bmatrix} \begin{bmatrix} \sigma_s \\ \sigma_y \\ \sigma_{xy} \end{bmatrix}_{\mathbf{P_b}} = \begin{bmatrix} \sigma_n \\ \sigma_t \end{bmatrix}_{\mathbf{P_b}}, \tag{22a}$$

or:

$$\mathbf{T}^*\boldsymbol{\sigma} = \boldsymbol{\sigma}^*. \tag{22b}$$

Substituting the constitutive Equation 4 into Equation 22b gives the following:

$$\mathbf{T}^*\mathbf{D}\boldsymbol{\varepsilon} = \boldsymbol{\sigma}^*, \tag{23}$$

where vector $\boldsymbol{\varepsilon}$ represents strains at the point cell. The strains in Equation 23 can be approximated using a 4-node interim element, whose vertices are the center of adjacent internal cell $\mathbf{P}$, point cell $\mathbf{P_b}$ and the nodes lying at either side of the point cell (Figure 3a). It is noticeable that the 4-node interim element corresponding to a point cell has three nodes which are located on a straight boundary face. In such a node arrangement, one of the internal angles of the interim element becomes 180 degrees, which is the upper limit for an internal angle of a linear element [12]. Substituting Equation 12 into Equation 23 gives the following:

$$\mathbf{T}^*\mathbf{D}\mathbf{B}\widetilde{\mathbf{u}} = \boldsymbol{\sigma}^*. \tag{24}$$

Matrix $\mathbf{B}$ in Equation 24 can be approximated at the centre of the interim element in the corresponded natural coordinate system. It is noticeable that this approximated evaluation is also utilized in Equation 13b for the face of an internal cell that lies on the boundary of the domain. Each individual equation in Equation 24 includes the displacement components of the nodes at either side of the point cell, which must be eliminated. The elimination procedure is similar to that used in Equation 19 for the internal cells. Consequently, equations, which relate the unknown displacements at point cell $\mathbf{P_b}$ to the displacements at the centres of the surrounding cells and to the applied stresses, will be obtained. These equations are also in the form of Equation 20, with a nonzero right hand side. Moreover, in the case of mixed boundary conditions, a proper combination of individual equations taken from Equations 21 and 24 is used.

SOLUTION PROCEDURE

As mentioned in the preceding sections, stresses corresponding to the cell faces are approximated, using the values of the shape functions of the interim elements. For a given interim element, the natural coordinates of the evaluation point can be corresponded to the middle of the enclosed face and the centre of the interim element. To preserve the simplicity of the method, the centres of the interim elements, i.e. $r = s = 0$, are used as the evaluation points in the following test cases.

Equation 20, corresponding to the internal cells and equations from the boundary conditions, provides a system of simultaneous linear equations containing all of the unknown displacements and can be expressed in the matrix form as follows:

$$\mathbf{AX} = \mathbf{C}. \tag{25}$$

A is a non-symmetric sparse matrix and contains the coefficients relating the unknown displacements associated with the cells. **X** is a vector including the unknown variables and vector **C** represents the known values on the boundaries. Equation 25 can be solved by an appropriate solver technique, such as the bi-conjugate gradient method, which is employed here to yield the displacements of the solution domain.

NUMERICAL EXAMPLES

The procedure proposed in this paper has been implemented in the FORTRAN computer code and applied to three test cases, including an internally pressurized thick-walled cylinder, a tapered panel, known as 'Cook's membrane problem' and a cantilever beam subjected to a uniformly distributed direct load. The method's accuracy has been assessed by comparing the predicted results with analytical and numerical results reported in the literature. The convergence behaviour towards the analytical solution has been studied in the first test problem to show the convergence rate of the present discretization method.

Test Case-1

The first test concerns a thick-walled cylinder loaded by a uniform internal pressure. The ends of the cylinder are unconstrained and open, which experiences a symmetric deformation about the axial axis. A unit length, with a 3 mm inner radius and a 6 mm outer radius, is considered. The material properties are given in Figure 4. The problem is considered under a plane stress condition. Due to the symmetric nature of the problem, only one quarter of the cylinder is modelled and meshed to the quadrilateral elements and symmetric boundary conditions are applied. Figure 4 shows one quarter of the cylinder, which is meshed to

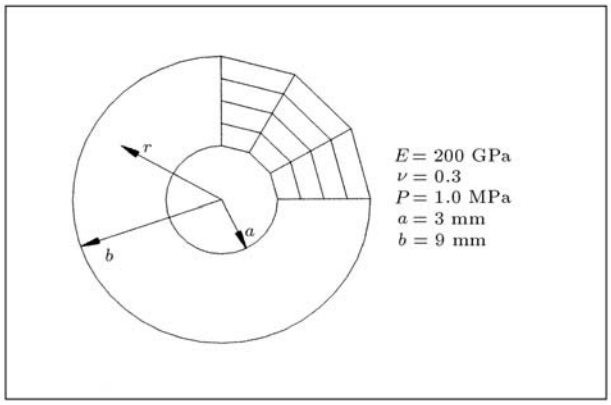

Figure 4. One quarter of the thick-walled cylinder meshed to 3 × 4.

3×4, i.e., three elements in the circumferential direction and four elements in the radial direction. Hoop and radial stresses are calculated, which are the principal stresses, due to symmetry in the cylinder.

The effect of mesh refinement on the accuracy of the results is illustrated in Figure 5. The refinement is performed at two levels and the cylinder is analyzed. The principle stresses, along a central line that passes through the thickness of the cylinder, are compared with the analytical solutions. As Figure 5 shows, the results converge to the analytical solutions, as the mesh gets finer. Furthermore, the radial displacements are evaluated at the cells centres, corresponding to the 6 × 8 mesh density. The results are compared with the analytical solutions given by Ugural and Fenster [13] in Figure 6. This figure depicts the capability of the presented formulation in prediction of the displacement field.

A convergence study for stress error is performed on the same cylinder test problem. One quarter of the

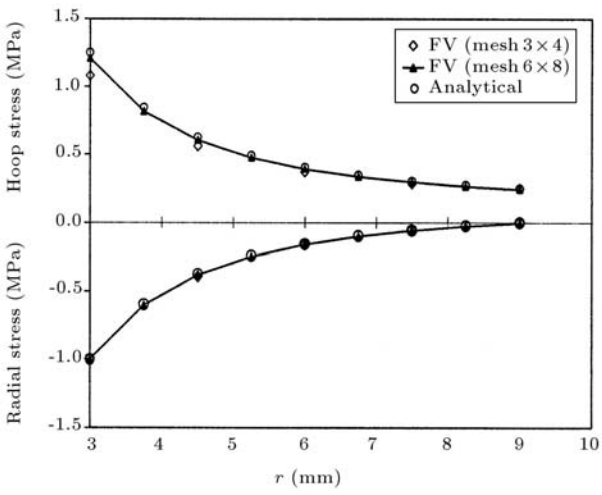

Figure 5. Distribution of principle stresses in a thick-walled cylinder subjected to internal uniform pressure.

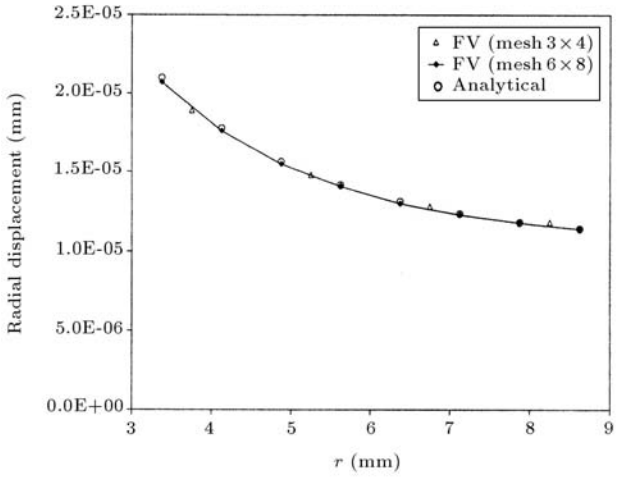

Figure 6. Distribution of radial displacement in a thick-walled cylinder subjected to internal uniform pressure.

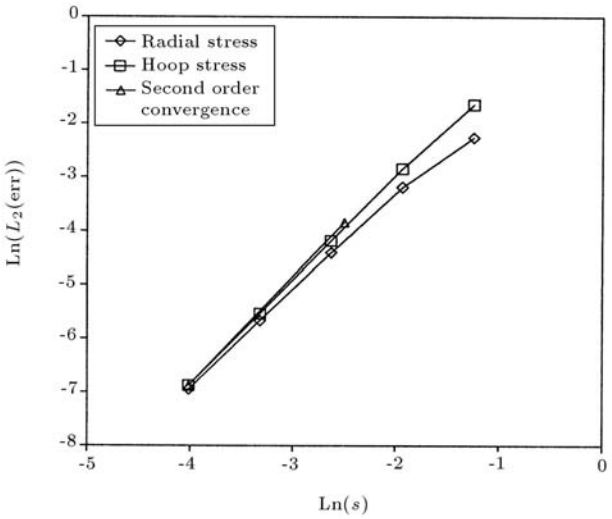

Figure 7. Convergence of the stress error norms for the thick-walled cylinder.

cylinder is meshed to $N = 3 \times 4$, $N = 6 \times 8$, $N = 12 \times 16$, $N = 24 \times 32$ and $N = 48 \times 64$ elements, using quadrilateral elements. The normalized L_2 stress error norms are calculated for the radial and hoop stresses, using the following equation:

$$L_2(\mathrm{err})_\sigma = \sqrt{\frac{\sum_{i=1}^{\mathrm{totface}} (\sigma - \sigma^{fv})_i^2}{\sum_{i=1}^{\mathrm{totface}} \sigma_i^2}}, \tag{26}$$

where σ and σ^{fv} denote the analytical and the finite volume solutions corresponding to the cell faces, respectively. The parameter, 'totface', in Equation 26, indicates the total number of cell faces of the model. A characteristic mesh size, s, is obtained in the following form:

$$s = \frac{1}{\sqrt{N}}, \tag{27}$$

where N is the total number of elements. Figure 7 shows the convergence rate towards the analytical results for the meshes used. As seen in this figure, the convergence rate for the solutions obtained is comparable with the second order behaviour.

Test Case-2

As a second test, a tapered panel, clamped at one end, is considered. This problem is often referred to as 'Cook's membrane problem', and was proposed to assess the distortion capability of the formulations. The geometry and the material properties are shown in Figure 8. The right end of the panel is subjected to a unit load, which is uniformly distributed along the

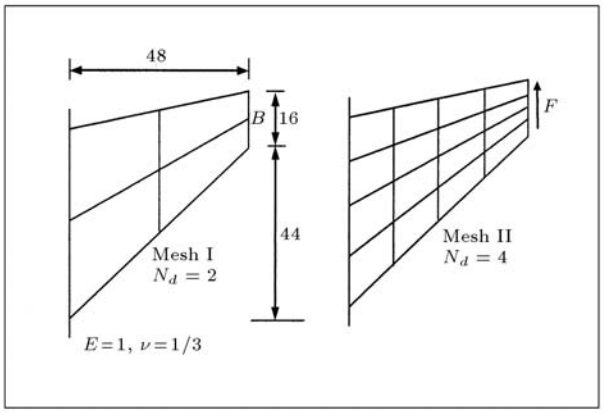

Figure 8. Cook's membrane problem with unit load uniformly distributed along right edge.

edge. The panel is meshed to 2×2, 4×4 and 16×16, two of which are shown in Figure 8. The presented method and the CV-FVM method were used for the plane stress analysis of the problem. The results obtained for the vertical displacement at B are shown in Table 1. The results of the finite element analysis are also shown in Table 1, which is taken from [14]. The results of the CV-FVM approach are obtained from a code, which was originally developed at Greenwich University by Professor Bailey [6] and which was, then, extended by Fallah [7] to include the geometric non-linearity effects. It can be seen that the results of the presented method are comparable to the results predicted by the finite elements. It is also seen that the CV-FVM predictions are less than the predictions of the presented method in coarse meshes. However, the results of CV-FVM are in good agreement with the Q4 finite element results. It should be noted that the presented method involves more degrees of freedom, shown in Table 1 as 'dof' in

Table 1. Finite element and finite volume predictions for the vertical displacement at B in Cook's problem.

	Element	$N_d = 2$	$N_d = 4$	$N_d = 16$
Finite Element [14]	HL	18.17	22.03	23.81
	HG	22.32	23.23	23.91
	Q4	11.85	18.30	23.43
	Q6	22.94	23.48	–
	QM6	21.05	23.02	–
Finite Volume	CV-FVM	11.23 (dof=18)	17.66 (dof=50)	23.34 (dof=578)
	CC-FVM	18.34 (dof=24)	20.71 (dof=64)	23.95 (dof=640)

the parenthesis, than the CV-FVM counterpart for the models of the same mesh.

The amount of CPU time used by the FV methods is very small in this test and their use is not convenient for comparison purposes. However, due to the non-symmetric nature of the coefficient matrix, it is expected that the FV methods spend more CPU time than its FE counterpart. In [6,15], the CPU time comparisons have been performed in favour of the FE method.

Test Case-3

As the final test, a cantilever beam, subjected to a uniformly distributed transverse load, is considered for the analysis. The geometry of the beam and the material properties are given in Figure 9. The presented formulation and a standard, in-house displacement based, finite element code are used in this test, where the plane stress conditions are assumed. The beam is meshed to 4-node quadrilateral elements, where the linear displacements were considered as unknown variables in both methods. It is well known that the modelling of a beam with a dominated bending deformation, by such quadrilateral elements, is inefficient. However, the purpose of the test is a comparison between the ability of the presented method and the ability of the standard finite element method in this modelling.

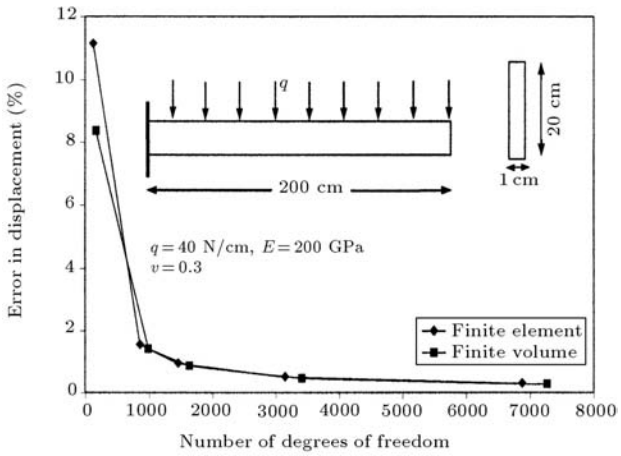

Figure 9. Error in prediction of tip displacement of a cantilever beam subjected to a uniformly distributed direct load.

Isoparametric formulation is used in the finite element method and, also, full integration is performed for the computation of element matrices. The beam is meshed to rectangular elements and progressively refined along the length and height of the beam. Moreover, the same meshes are used in both methods.

Using the same mesh density, finite volume has more degrees of freedom than the finite element counterpart, due to the introduction of point cells on the boundaries. Error in the value of tip displacement, predicted by both methods, is illustrated in Figure 9. The error is normalized, with respect to the analytical solution given by Timoshenko and Gere [16], which includes the shear effects on the tip displacement. The figure reveals that the finite volume results are as accurate as the finite element results, although, as expected, the finite volume presents slightly more accurate results than the finite element, due to using more degrees of freedom in the same mesh density.

CONCLUSION

In this paper, a method has been developed for approximating the displacement gradients at the cell faces of control volumes in a cell centred, finite volume framework, by use of an isoparametric element formulation. The procedure has been fully described in the matrix form and has been applied to three test cases. The capability of the proposed method in good prediction of stresses and deformations has been demonstrated by comparing the results obtained with the analytical and numerical results. Furthermore, the convergence rates towards the analytical solutions have been studied in the first test problem. The results have revealed behaviour comparable with the second order rate of convergence. While the proposed approach concerns two-dimensional linear elastic problems, on-going work is being undertaken to investigate the extension of this

approach to complex structural problems, i.e. complexity in terms of geometry and governing equations.

REFERENCES

1. Fallah, N. "Cell vertex and cell centred finite volume methods for plate bending analysis", *Computer Methods in Applied Mechanics and Engineering*, **193**, pp 3457-3470 (2004).
2. Demirdzic, I. and Martinovic, D. "Finite volume method for thermo-elasto plastic stress analysis", *Computer Methods in Applied Mechanics and Engineering*, **109**, pp 331-349 (1993).
3. Demirdzic, I. and Muzaferija, S. "Finite volume method for stress analysis in complex domains", *Int. J. Numer. Methods in Eng.*, **37**, pp 3751-3766 (1994).
4. Wheel, M.A. "A geometrically versatile finite volume formulation for plane elastostatic stress analysis", *Journal of Strain Analysis*, **31**(2), pp 111-116 (1996).
5. Wheel, M.A. "A mixed finite volume formulation for determining the small strain deformation of incompressible materials", *Int. J. Numer. Methods Eng.*, **44**(12), pp 1843-1861 (1999).
6. Bailey, C. and Cross, M. "A finite volume procedure to solve elastic solid mechanics problems in three dimensions on an unstructured mesh", *Int. J. Numer. Methods in Eng.*, **38**, pp 1757-1776 (1995).
7. Fallah, N.A., Bailey, C., Cross, M. and Taylor, G.A. "Comparison of finite element and finite volume methods application in geometrically nonlinear stress analysis", *Applied Mathematical Modelling*, **24**, pp 439-455 (2000).
8. Fallah, N.A. "Computational stress analysis using finite volume methods", Ph.D Thesis, The University of Greenwich, London, UK (2000).
9. Taylor, G.A., Bailey, C. and Cross, M. "A vertex-based finite volume method applied to non-linear material problems in computational solid mechanics", *Int. J. Numer. Methods in Eng.*, **56**, pp 507-529 (2003).
10. Patankar, S.V., *Numerical Heat Transfer and Fluid Flow*, McGraw-Hill (1989).
11. Bathe, K.J., *The Finite Element Procedures*, McGraw-Hill (1996).
12. Strang, G. and Fix, G.J., *An Analysis of the Finite Element Method*, Prentice Hall (1973).
13. Ugural, A.C. and Fenster, S.K., *Advanced Strength and Applied Elasticity*, Prentice Hall (1993).
14. Taylor, R.L., Beresford, P.J. and Wilson, E.L. "A non-conforming element for stress analysis", *Int. J. Numer. Methods Eng.*, **10**, pp 1211-1219 (1976).
15. Oñate, E., Cervera, M. and Zienkiewicz, O.C. "A finite volume format for structural mechanics", *Int. J. Numer. Methods Eng.*, **37**, pp 181-201 (1994).
16. Timoshenko, S.P. and Gere, J.M. "Mechanics of material", *Van Nostrand Reinhold* (1973).